

Comment on “Orthorhombic Symmetry and Anisotropic Properties of Rutile TiO₂”

Andreas Leineweber*

J. Phys. Chem. C **2023**, *127* (38), 19240–19249. DOI: [10.1021/acs.jpcc.3c04573](https://doi.org/10.1021/acs.jpcc.3c04573)

J. Phys. Chem. C **2026**, *130*. DOI: [10.1021/acs.jpcc.6c01057](https://doi.org/10.1021/acs.jpcc.6c01057)



Cite This: <https://doi.org/10.1021/acs.jpcc.5c08786>



Read Online

ACCESS |

 Metrics & More

 Article Recommendations

Recently, Gonzales Szwacki et al.¹ investigated the crystal structure of the rutile form of TiO₂ (rutile-TiO₂²) at ambient conditions (“room temperature” and normal pressure) and temperatures below. This was done based on evaluation of powder X-ray and neutron diffraction (PXRD and PND) experiments and based on first-principles calculations on structures (pertaining to the nonvibrating material at 0 K). The authors¹ concluded that at these ambient conditions, rutile-TiO₂ has the orthorhombic CaCl₂-type structure (Strukturbericht notation C35) with *Pnmm* space group symmetry instead of the classical rutile-type structure (Strukturbericht notation C4) with *P4₂/mnm* symmetry.² The main arguments were characteristically *hkl*-dependent peaks widths in the PXRD/PND data, which were attributed to reflection-splitting in accordance with lattice-parameters values $a \neq b$, discarding an alternative interpretation in terms of anisotropic microstrain broadening. Characteristic displacements of the O atoms appear to accompany the lattice distortion when evaluating the PXRD/PND data in terms of the CaCl₂-type structure. Moreover, the first-principles calculations seemed to imply that orthorhombic atomic geometries can have lower energies than more highly symmetric tetragonal ones.

The tetragonal rutile-type structure of rutile-TiO₂ is an iconic inorganic structure type.³ Its invalidation under ambient conditions would affect textbook knowledge. Indeed, already Tomei and Goletti⁴ questioned the conclusion of an orthorhombic CaCl₂-type structure based on undetectable effects predicted for some optical properties. In their reply, the original authors⁵ acknowledged “lower optical effects”, and once again emphasized their theoretical and experimental findings. Moreover, the authors addressed the relevance of domains in orthorhombic rutile-TiO₂, which obstructed macroscopic measurements.

In the present comment, the author more generally questions the interpretation of their PXRD/PND data by Gonzales Szwacki et al.¹ in terms of presence of a CaCl₂-type TiO₂. The present author acknowledges to be able to reproduce the results of the Rietveld refinements from ref 1 based on the published diffraction data as it concerns both the CaCl₂-type structure model and the alternatively presented rutile-type structure model with anisotropic microstrain broadening. The main point of this comment is that in the view of the present author, the latter tetragonal structure model with anisotropic microstrain broad-

ening should be regarded as the more appropriate one. The main argument is the bigger scientific context on rutile-TiO₂ and the typical characteristics of ferroelastic phase transformations.

In all this, the present author focuses to a lesser extent on the results of the first-principles calculations by Gonzales Szwacki et al.¹ Nevertheless, it is emphasized that the maximum determined energy difference between the, respectively, lowest-energy CaCl₂-type and rutile-type state amounts to only 1.5 meV/atom and lower values, depending strongly on the calculation settings. In terms of thermal energy, 1.5 meV/atom corresponds to 17 K. Even if these results would be valid, a CaCl₂-type energy minimum would occur twice ($a < b$ and $b < a$) in the form of a double-well minimum in the lattice-parameter/atomic displacement space with a rutile-type saddle point ($a = b$). The corresponding detailed energy landscape has not been explored by Gonzales Szwacki et al.,¹ as it had, e.g., been done in an earlier work on isotypic β -PbO₂.⁶ In that work a similar energy difference was encountered by first-principles calculations, and it was suggested that such a double-well potential is dynamically averaged out toward a rutile-type β -PbO₂ at room temperature. Hence, even if the first-principles calculations indicate that a low-symmetry orthorhombic CaCl₂-type energy minimum for rutile-TiO₂ has a lower energy than any other high-symmetry tetragonal rutile-type state, this may be averaged out by phonons at $T > 0$ K or even at $T = 0$ K (zero-point vibrations). In any case, the first-principles calculations by Gonzales Szwacki et al.¹ contrast a series of other detailed first-principles calculations on rutile-TiO₂ in the literature. Such calculations did not only predict the rutile-type structure to be stable at 0 K at 0 GPa but, more importantly, also a transition rutile-type \rightarrow CaCl₂-type at an elevated pressure of $p^* = 7.6\text{--}13$ GPa.^{7–9} Such a transition at room temperature and elevated pressure had already been predicted by extrapolating pressure-dependent elastic constants.¹⁰ Experimentally, this transition has not yet been verified likely due to competing structural transitions observed

Received: December 31, 2025

Revised: April 2, 2026

Accepted: April 2, 2026

for TiO₂,¹¹ as also pointed out in one of the afore-cited theoretical works.⁷

Some bigger context for the question for the discussed transition *rutile-type* → *CaCl₂-type* structure for rutile-TiO₂ is provided by comparison with the pressure-dependent structural behavior of other dioxides and difluorides, which have a traditionally well-established *rutile-type* structure at ambient conditions: e.g., stishovite-SiO₂,^{12,13} GeO₂,^{14,15} SnO₂,¹⁶ β-PbO₂,¹⁷ NiF₂, (β-)MnO₂,^{16,18} MgF₂.^{16,19} appear to show phase transitions to a *CaCl₂-type* structure at room temperature and elevated pressure. Only for a few chlorides and bromides, for which the *CaCl₂-type* structure appears to exist at ambient conditions, does the transition toward a *rutile-type* structure occur at an elevated temperature *T**: e.g., CaCl₂ and CaBr₂.^{20,21} Taking stishovite-SiO₂ as a model, the typical course of the *rutile-type* → *CaCl₂-type* was modeled within Landau theory as a second-order pseudoproper ferroelastic phase transition, which involves a necessary symmetry change.^{22,23} An excellent agreement with experimental data could be demonstrated.^{12,13,22} Independently of the *rutile/CaCl₂-type* structured material, it appears that the *CaCl₂-type* polymorph gets stabilized over the *rutile-type* polymorph with increasing pressure and decreasing temperature.

The main point to be made under the above-mentioned context is that the existence of a *CaCl₂-type* TiO₂ at room temperature and normal pressure as proposed by Gonzalez Szwacki et al.¹ contradicts occurrence of a transition *rutile-type* → *CaCl₂-type* at 0 K^{7–9}/room temperature¹⁰ and, respectively, elevated pressure *p**. Hence, the low-pressure state should not be orthorhombic. This contradiction also sheds new light on earlier works (and actually invalidates them) involving some of the authors of ref 1, which had proposed presence of a *CaCl₂-type* structure at ambient conditions based on similar powder diffraction evidence (mainly PXRD). In these works, even direct experimental evidence for the ferroelastic transitions at elevated pressure exist: The first work was on (β-)MnO₂,²⁴ where a *rutile-type* → *CaCl₂-type* transition was reported to occur in other works at 0.3–1.9 GPa¹⁸ and later at 4 GPa,¹⁶ using refined data evaluation methodology. The second work was on β-PbO₂,²⁵ where a corresponding transition had been reported at 4 GPa.¹⁷

After objecting against a *CaCl₂-type* structure for rutile-TiO₂ at ambient conditions based on the general pressure- and temperature-dependent behavior of rutile-TiO₂ and of similar systems, now the refined structural parameters by Gonzalez Szwacki et al.¹ will be scrutinized. This is done in terms of two parameters used already in that work, which are illustrated in Figure 1. The metrical distortion *r_{ab}* (basically quantifying spontaneous strain) is calculated from the orthorhombic lattice parameters *a* and *b*:

$$r_{ab} = 2 \frac{a - b}{a + b} \quad (1)$$

The second parameter *r_{xy}* accounts for the rotation of the O-octahedra around the Ti atoms and quantifies the difference between the fractional coordinates *x* and *y* of the O atoms as illustrated in Figure 1:

$$r_{xy} = 2 \frac{x - y}{x + y} \quad (2)$$

Whereas *r_{ab}* = *r_{xy}* = 0 holds in the *rutile-type* structure, in all considered *CaCl₂-type* structures, they assume the same sign. The states with (*r_{ab}*, *r_{xy}*) = −(*r_{ab}*, *r_{xy}*) are rotated by 90°; i.e., they

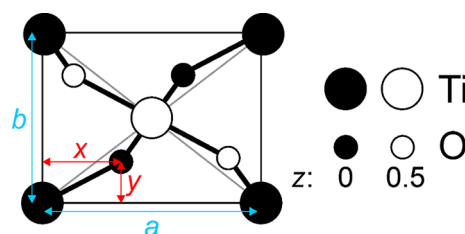


Figure 1. Unit cell of an orthorhombic *CaCl₂-type* structure of TiO₂, shown as the distribution of the atoms within a unit cell viewed downstream [001]. The lattice parameters *a* and *b* as well as the fractional coordinates *x* and *y* are basis calculation of the parameters *r_{ab}* and *r_{xy}* (eqs 1 and 2). In the special case of the tetragonal *rutile-type* structure, *a* = *b* and *x* = *y* (*r_{ab}* = *r_{xy}* = 0) with the latter implying that the O atoms are located on the gray lines. With considerable changes adapted from and redrawn according to ref 1. Copyright 2022 American Chemical Society.

represent the same structures and in a real microstructure they can be considered to represent orientational domain states, corresponding to the two equivalent minima in a double-well potential as mentioned above and previously considered in ref 6. In the following, *a* > *b* is adopted and thus *x* > *y*, i.e., resulting in positive *r_{ab}*, *r_{xy}*. Data from the literature on some dioxides used for comparison are transformed accordingly.

Figure 2 depicts the values of (*r_{ab}*, *r_{xy}*) for a series of structure determinations at elevated pressures or some dioxides from the

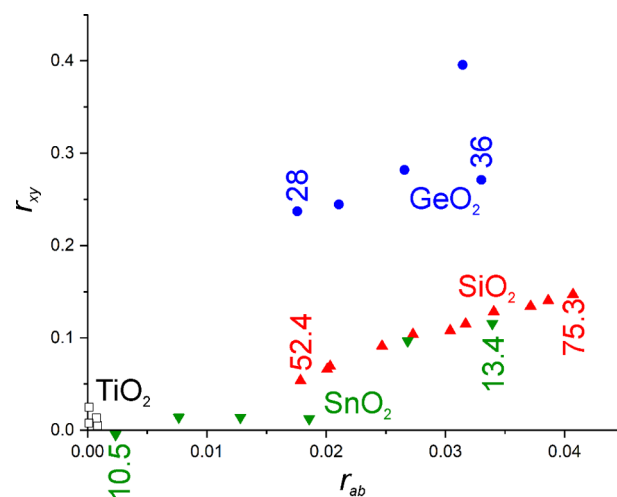


Figure 2. Distortion parameters *r_{ab}* (eq 1) and *r_{xy}* (eq 2) as determined experimentally from X-ray powder diffraction data taken at ambient conditions from rutile-TiO₂ (squares) and adopting a *CaCl₂-type* structure (Table 7 of ref 1). These data are contrasted with pressure-dependent data (at normal temperature) taken above the *rutile-type* → *CaCl₂-type* transition pressures *p** from SiO₂¹³ (*p** = 51.4 GPa; red triangles), GeO₂¹⁵ (*p** = 25 GPa; blue circles), and SnO₂¹⁶ (*p** = 10.3 GPa; green inverted triangles). The, respectively, highest and lowest pressures are indicated by the numbers in GPa. The lowest pressure of each set of data pertaining to the *CaCl₂-type* phase is larger than the respectively assessed value of *p** due to the discrete character of the pressures at which the diffraction data were measured.

literature as well as determined¹ for TiO₂ based on PXRD at ambient conditions. The latter values are much smaller than most of the pressure-dependent values. This does not automatically invalidate the values for TiO₂,¹ but the smallness of these values may raise the suspicion that they are of a different character than the larger values.

The data from the other dioxides in Figure 2 correspond to values recorded at pressures above the pressure p^* of the ferroelastic *rutile*-type \rightarrow *CaCl₂*-type phase transitions occurring with increasing pressure (or decreasing temperature; not included in Figure 2). According to the above-mentioned Landau-theory description of the transition,²² there should be a bilinear coupling of the atomic distortions (the primary order parameter; corresponding to r_{xy}) and the orthorhombic distortion (the spontaneous strain; here corresponding to r_{ab}). Hence, above the transition pressure p^* (or below the transition temperature T^*) the values are expected to vary according to $r_{xy} \sim r_{ab} \sim [T^* - T]^{1/2} \sim [p - p^*]^{1/2}$ in the orthorhombic structure, while they are both 0 in the tetragonal structure. Furthermore, approaching the transition from the tetragonal state from below p^* (above T^*) the shear modulus $C' = \frac{1}{2}(C_{11} - C_{12})$ (C_{11} , C_{12} being the components of the 6×6 Voigt stiffness matrix) approaches 0; beyond the transition, the modulus $\frac{1}{4}(C_{11} + C_{22} - 2C_{12})$ pertaining to the orthorhombic structure increases from 0 to adopt increasingly positive values. Accordingly, corresponding shear deformations become more and more easy within the tetragonal phase approaching the transition, but the corresponding pronounced elastic anisotropy may also exist quite far from the transition. However, it has to be emphasized that the Landau-theory-based description of the pressure- or temperature-dependent crystal structure including the phase transition corresponds to a mean-field description of the intrinsic crystal structure. Hence, this description excludes effects due to (extrinsic) defects/heterogeneities and effects due to critical fluctuations.

Comparing the (r_{ab}, r_{xy}) values determined for rutile-TiO₂ by Gonzalez Szwacki et al.¹ with the pressure-dependent values of the other dioxides at pressures above the *rutile*-type \rightarrow *CaCl₂*-type phase transition, the small values for rutile-TiO₂ are only expected very close to the phase transition. This would imply that with decreasing temperature or with increasing pressure, one would expect much larger values. Reports on structure data do not indicate such behavior, including low-temperature data by Gonzalez Szwacki et al.¹ (especially as it concerns the values for r_{ab} ; see their Table 6). In any case, as already stated above, there is experimental and theoretical evidence that the true ferroelastic transition for rutile-TiO₂ should occur at *elevated* pressures.^{7–10}

In view of the preceding considerations, it is now suggested that at ambient conditions, rutile-TiO₂ indeed exhibits the long-established tetragonal *rutile*-type structure. Consequently, the anisotropic line broadening interpreted in terms of a *CaCl₂*-type structure model Gonzalez Szwacki et al.¹ and corresponding tiny reflection splitting, should instead be interpreted microstructure-induced anisotropic microstrain. Such model was discarded by Gonzalez Szwacki et al.¹ Elastic microstress is expected to occur as soon as there are local structural misfits in a microstructure, e.g., due to misfitting grains or due to dislocations.^{26,27} The corresponding microstress-induced microstrain is expected to more or less exhibit the material's elastic anisotropy, e.g., by showing a direction dependence of the line widths qualitatively similar to the reciprocal of Young's modulus, $1/E$.^{26,27} Conventional values of the experimental elastic constants determined at ambient conditions adopting standard tetragonal symmetry²⁸ imply $C' = \frac{1}{2}(C_{11} - C_{12}) = 46$ GPa, which is small but well positive. The next larger shear modulus resulting from eigenvalue/eigenvector analysis of the stiffness

matrix corresponds to $C_{44} = C_{55} = 124$ GPa. The direction dependence of $1/E$ as shown in Figure 3 agrees with the broad

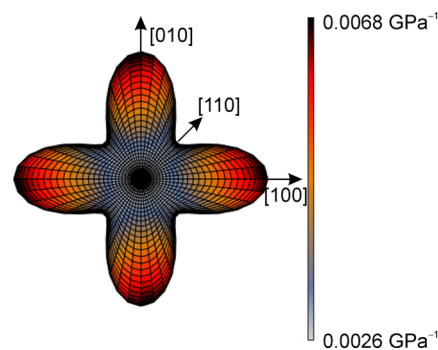


Figure 3. Projection of the tensor surface of the direction-dependent reciprocal Young's modulus, $1/E$ of rutile-TiO₂ calculated using elastic constants determined for ambient conditions adopting tetragonal symmetry,³⁷ implying $E(100) = 148$ GPa, $E(110) = 373$ GPa, and $E(001) = 384$ GPa. The large values of $1/E$ along the $[100]$ is strongly connected with the small value of $C' = 1/2(C_{11} - C_{12})$ and is the main reason for the pronounced anisotropy of the microstrain broadening (see text).

$h00$ and narrow $hh0$ Bragg reflections as reported by Gonzalez Szwacki et al.¹ and which was the basis for the proposal of orthorhombicity by these authors. However, it has been shown by the present author that in the limit of small distortions microstrain broadening and reflection splitting can lead to virtually the same diffraction patterns,²⁹ suggesting that other means are required to justify choice of the appropriate model. It is the strong theoretical evidence for elastic instability of *rutile*-type TiO₂ and of other oxides and fluorides at *elevated pressures* described above, which excludes the presence of the *CaCl₂*-type structure also at normal pressure.

Anisotropic microstrain broadening has been studied for materials exhibiting a ferroelastic *tetragonal* \rightarrow *orthorhombic* phase associated with a small value of C' in the tetragonal phase. Notable examples are As₂O₅,³⁰ showing a transition with decreasing T or Pb₃O₄³¹ upon following the transition with increasing pressure. In the case of As₂O₅ the temperature evolution of (true) orthorhombic splitting below the assessed transition temperature was shown to be well compatible with Landau theory adopting a second-order proper ferroelastic transition. As argued above, the line broadening present above the transition temperature T^* can only be attributed to anisotropic line broadening, as also done in ref 30. While in that work the broadening was associated with critical fluctuations, it has been argued by other authors that ferroelectric (and ferroelastic) materials behave largely according to the mean-field approximation such that critical fluctuations should be negligible.^{32,33} Instead, emergence of apparently critical behavior in such materials were instead attributed to defects/heterogeneities in the material.³² Such *extrinsic* defects and heterogeneities are expected to be omnipresent in real materials. As already described above for the case of rutile-TiO₂, if such defects induce *local elastic strains* aka microstrain, this microstrain will reflect the elastic anisotropy, e.g., in the form of microstrain broadening with hkl dependence mainly in agreement with direction dependence of the reciprocal Young's modulus (see also above). That modulus is strongly influenced by the small value of C' which

approaches 0 when approaching the phase transition from the tetragonal side.^{22,23}

As formulated by Stephens,³⁴ microstrain broadening can be conceived as resulting from a correlated distribution of lattice parameters (formulated in terms of the components of the reciprocal metrical tensor) for *whatever reason* around an average, which is regarded as the true lattice parameter. In view of the present picture, the reason for microstrain is local microstresses (for the influence of macrostresses which may be generated in a diamond anvil cell and which might strongly influence the encountered broadening see Singh³⁵). Hence, the “orthorhombic” crystallites apparently generating the orthorhombic distortion are caused by deviatoric stresses. The resulting elastic strains are well expected to be accompanied by displacements of the O atoms as reflected by the refined r_{xy} values¹ so that this effect can well be reconciled with a truly tetragonal *rutile*-type structure of the material unaffected by the microstress. Thereby, the displacements of the O atoms caused by an elastic strain can be regarded as a deviation from the Cauchy–Born approximation stating that the internal atomic structure follows an elastic strain in a homogeneous fashion.³⁶ In any case, observing such displacements for (elastically) strained TiO₂ provides no independent support for an intrinsically orthorhombic crystal structure.

The present example highlights the importance of acknowledging that the diffraction pattern of some crystalline specimens always reflects its *real structure*. This real structure is a combination of what should be regarded as the actual *intrinsic* crystal structure (including equilibrium point defects) which may be a true minimization of Gibbs energy and *extrinsic*, nonequilibrium *microstructure*, as finite crystallite size, extended faults as dislocations and planar faults. The microstructure can cause diffraction line broadening and more complicated diffraction effects.^{38,39} In some cases, such as the present one of rutile-TiO₂, the diffraction effects due to microstructure, e.g., anisotropic microstrain broadening, can be in principle be modeled empirically by modifying the model for the intrinsic crystal structure. However, this leads to a crystal structure model inappropriately representing the material’s energy landscape. Taking this into account in the present work, the appropriate model of the intrinsic crystal structure for rutile-TiO₂ was argued to be the classical tetragonal *rutile*-type structure rather than the orthorhombic *CaCl₂*-type structure. The line broadening should be attributed as defect/microstress-induced microstrain, where the anisotropy of the broadening is compatible with the well-known elastic anisotropy of (tetragonal) rutile-TiO₂.

AUTHOR INFORMATION

Corresponding Author

Andreas Leineweber – Institute of Materials Science, TU Bergakademie Freiberg, 09599 Freiberg, Germany;
orcid.org/0000-0002-8948-8975;
Email: andreas.leineweber@iww.tu-freiberg.de

Complete contact information is available at:
<https://pubs.acs.org/10.1021/acs.jpcc.5c08786>

Notes

The author declares no competing financial interest.

ACKNOWLEDGMENTS

The authors thanks Dr. Christian Schimpf, Institute of Materials Science, Technical University Bergakademie Freiberg for preparing Figure 3.

REFERENCES

- (1) Gonzalez Szwacki, N.; Fabrykiewicz, P.; Sosnowska, I.; Fauth, F.; Suard, E.; Przenioslo, R. Orthorhombic Symmetry and Anisotropic Properties of Rutile TiO₂. *J. Phys. Chem. C* **2023**, *127* (38), 19240–19249.
- (2) The notion rutile-TiO₂ refers to the type of titanium dioxide with the corresponding octahedral connectivity irrespective of the actual symmetry. The notions *CaCl₂*-type and *rutile*-type structure (using italics) refer to the crystal structure types with respective symmetry.
- (3) Baur, W. H. The rutile type and its derivatives. *Crystallogr. Rev.* **2007**, *13* (1), 65–113.
- (4) Tomei, I.; Goletti, C. Comment on “Orthorhombic Symmetry and Anisotropic Properties of Rutile TiO₂”. *J. Phys. Chem. C* **2025**, *129* (25), 11809–11810.
- (5) Gonzalez Szwacki, N.; Fabrykiewicz, P.; Sosnowska, I.; Fauth, F.; Suard, E.; Przenioslo, R. Reply to “Comment on ‘Orthorhombic Symmetry and Anisotropic Properties of Rutile TiO₂’”. *J. Phys. Chem. C* **2025**, *129* (25), 11811–11812.
- (6) Chen, T.; Shao, D.; Lu, P.; Wang, X.; Wu, J.; Sun, J.; Xing, D. Anharmonic effect driven topological phase transition in PbO₂ predicted by first-principles calculations. *Phys. Rev. B* **2018**, *98* (14), No. 144105.
- (7) Montanari, B.; Harrison, N. M. Pressure-induced instabilities in bulk TiO₂ rutile. *J. Phys.: Condens. Matter* **2004**, *16* (3), 273.
- (8) Lukačević, I.; Gupta, S. K.; Jha, P. K.; Kirin, D. Lattice dynamics and Raman spectrum of rutile TiO₂: The role of soft phonon modes in pressure induced phase transition. *Mater. Chem. Phys.* **2012**, *137* (1), 282–289.
- (9) Liu, Y.; Jiang, Z.-Y.; Zhang, X.-D.; Wang, W.-X.; Zhang, Z.-Y. Deep-learning molecular dynamics simulation of pressure-driven transformation for bulk TiO₂. *Ceram. Int.* **2024**, *50* (20, Part A), 37900–37907.
- (10) Fritz, I. J. Pressure and temperature dependences of the elastic properties of rutile (TiO₂). *J. Phys. Chem. Sol.* **1974**, *35* (7), 817–826.
- (11) Gerward, L.; Staun Olsen, J. Post-Rutile High-Pressure Phases in TiO₂. *J. Appl. Crystallogr.* **1997**, *30* (3), 259–264.
- (12) Andrault, D.; Fiquet, G.; Guyot, F.; Hanfland, M. Pressure-Induced Landau-Type Transition in Stishovite. *Science* **1998**, *282* (5389), 720–724.
- (13) Zhang, Y.; Chariton, S.; He, J.; Fu, S.; Xu, F.; Prakapenka, V. B.; Lin, J.-F. Atomistic insight into the ferroelastic post-stishovite transition by high-pressure single-crystal X-ray diffraction. *Am. Mineral.* **2023**, *108* (1), 110–119.
- (14) Haines, J.; Léger, J. M.; Chateau, C.; Bini, R.; Ulivi, L. Ferroelastic phase transition in rutile-type germanium dioxide at high pressure. *Phys. Rev. B* **1998**, *58* (6), R2909–R2912.
- (15) Haines, J.; Léger, J. M.; Chateau, C.; Pereira, A. S. Structural evolution of rutile-type and *CaCl₂*-type germanium dioxide at high pressure. *Phys. Chem. Miner.* **2000**, *27* (8), 575–582.
- (16) Curetti, N.; Merli, M.; Capella, S.; Benna, P.; Pavese, A. Low-pressure ferroelastic phase transition in rutile-type AX₂ minerals: cassiterite (SnO₂), pyrolusite (MnO₂) and sellaite (MgF₂). *Phys. Chem. Miner.* **2019**, *46* (10), 987–1002.
- (17) Haines, J.; Léger, J. M.; Schulte, O. The high-pressure phase transition sequence from the rutile-type through to the cotunnite-type structure in PbO₂. *J. Phys.: Condens. Matter* **1996**, *8* (11), 1631.
- (18) Haines, J.; Léger, J. M.; Hoyau, S. Second-order rutile-type to *CaCl₂*-type phase transition in β -MnO₂ at high pressure. *J. Phys. Chem. Sol.* **1995**, *56* (7), 965–973.
- (19) Haines, J.; Léger, J. M.; Gorelli, F.; Klug, D. D.; Tse, J. S.; Li, Z. Q. X-ray diffraction and theoretical studies of the high-pressure structures and phase transitions in magnesium fluoride. *Phys. Rev. B* **2001**, *64* (13), No. 134110.

- (20) Howard, C. J.; Kennedy, B. J.; Curfs, C. Temperature-induced structural changes in CaCl_2 , CaBr_2 , and CrCl_2 : A synchrotron x-ray powder diffraction study. *Phys. Rev. B* **2005**, *72* (21), No. 214114.
- (21) Unruh, H.-G. Ferroelastic phase transitions in calcium chloride and calcium bromide. *Phase Transitions* **1993**, *45* (1), 77–89.
- (22) Carpenter, M. A.; Hemley, R. J.; Mao, H. High-pressure elasticity of stishovite and the $P4_2/mnm \rightleftharpoons Pnmm$ phase transition. *J. Geophys. Res.* **2000**, *105* (B5), 10807–10816.
- (23) Carpenter, M. A.; Salje, E. K. H. Elastic anomalies in minerals due to structural phase transitions. *Eur. J. Mineral.* **1998**, *10* (4), 693–812.
- (24) Fabrykiewicz, P.; Przenioslo, R.; Sosnowska, I.; Fauth, F.; Oleszak, D. Verification of the de Wolff hypothesis concerning the symmetry of $\beta\text{-MnO}_2$. *Acta Crystallogr., Sect. A* **2019**, *75* (6), 889–901.
- (25) Fabrykiewicz, P.; Przenioslo, R.; Szwacki, N. G.; Sosnowska, I.; Suard, E.; Fauth, F. Orthorhombic symmetry and anisotropic properties of $\beta\text{-PbO}_2$. *Phys. Rev. B* **2021**, *103* (6), No. 64109.
- (26) Leineweber, A. Understanding anisotropic microstrain broadening in Rietveld refinement. *Z. Kristallogr.* **2011**, *226* (12), 905–923.
- (27) Leineweber, A. Thermal expansion anisotropy as source for microstrain broadening of polycrystalline cementite, Fe_3C . *J. Appl. Crystallogr.* **2016**, *49* (5), 1632–1644.
- (28) Wachtman, J. B., Jr; Tefft, W. E.; Lam, D. G. JR. Elastic Constants of Rutile (TiO_2). *J. Res. Natl. Bur. Stand., Sect. A* **1962**, *66A*, 465.
- (29) Leineweber, A. Reflection splitting-induced microstrain broadening. *Powder Diffr.* **2017**, *32* (S1), S35–S39.
- (30) Redfern, S. A. T.; Salje, E. Spontaneous strain and the ferroelastic phase transition in As_2O_5 . *J. Phys. C: Solid State Phys.* **1988**, *21* (2), 277.
- (31) Leineweber, A.; Dinnebier, R. E. Anisotropic microstrain broadening of minium, Pb_3O_4 , in a high-pressure cell: interpretation of line-width parameters in terms of stress variations. *J. Appl. Crystallogr.* **2010**, *43* (1), 17–26.
- (32) Scott, J. F. Absence of critical exponents in ferroelectrics: experiments of Hilczer and theory of Levanyuk and Sigov. *Phase Transitions* **2016**, *89* (7–8), 645–650.
- (33) Salje, E. K. Ferroelastic Materials. *Annu. Rev. Mater. Res.* **2012**, *42*, 265–283.
- (34) Stephens, P. W. Phenomenological model of anisotropic peak broadening in powder diffraction. *J. Appl. Crystallogr.* **1999**, *32* (2), 281–289.
- (35) Singh, A. K.; Andrault, D.; Bouvier, P. X-ray diffraction from stishovite under nonhydrostatic compression to 70 GPa: Strength and elasticity across the tetragonal→orthorhombic transition. *Physics of the Earth and Planetary Interiors* **2012**, *208–209*, 1–10.
- (36) Ericksen, J. L. On the Cauchy—Born Rule. *Math. Mech. Solids.* **2008**, *13* (3–4), 199–220.
- (37) Manghnani, M. H. Elastic constants of single-crystal rutile under pressures to 7.5 kilobars. *J. Geophys. Res.* **1969**, *74* (17), 4317–4328.
- (38) Guinier, A. *X-Ray Diffraction: In Crystals, Imperfect Crystals, and Amorphous Bodies*; Dover Books on Physics; Dover Publications Incorporated, 1994.
- (39) Krivoglaz, M. A.; Baryakhtar, V. G.; Ivanov, M. A.; Moss, S. C.; Peisl, J. *X-Ray and Neutron Diffraction in Nonideal Crystals*; Springer: Berlin Heidelberg, 1996; DOI: 10.1007/978-3-642-74291-0.